

# Self-patterned H-bond supramolecular self-assembly

Y. W. Cao, X. D. Chai,\*<sup>a</sup> T. J. Li,<sup>a</sup> Jim Smith<sup>b</sup> and DeQuan Li\*<sup>b</sup>

<sup>a</sup> Department of Chemistry, Jilin University, Changchun, 10023, P. R. China

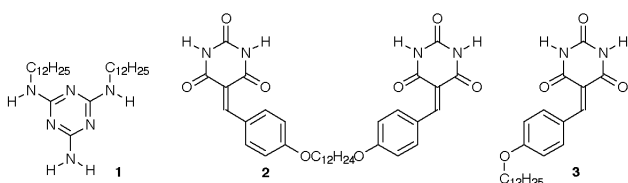
<sup>b</sup> Los Alamos National Laboratory, Chemical Sciences and Technology Division (CST-4), and Center for Materials Science, Los Alamos, NM 87545, USA. E-mail: dequan@lanl.gov

Received (in Columbia, MO, USA) 6th April 1999, Accepted 1st June 1999

**Barbituric acid and melamine derivatives self-assembled into highly ordered structures from the molecular scale ( $\sim 3$  Å) to geometric patterns on a macroscale ( $\sim 0.5$  mm).**

Supramolecular self-assembly is a fascinating process in which hierarchical organization from the molecular level to the mesoscale and macroscale is spontaneously established. Mesoscale ordered domains have been observed before,<sup>1</sup> but formation of well-defined patterns up to the macroscale is rare. Given knowledge of chemical functionalities, it is widely accepted that one cannot accurately predict the spontaneously organized structures by design, from intuition, or from physical principles. Here we attempt to understand the relationship between self-assembled structures and molecular functionalities using SEM, TEM, X-ray, and IR spectroscopy. Hydrogen bonding has long been employed as a powerful tool to organize molecules in the solid state<sup>2</sup> and on air/water interfaces.<sup>3</sup> H-bonded networks in barbituric acid and melamine systems<sup>4</sup> are intriguing because of their structural resemblance to the base pairs of DNA. We synthesized new derivatives of barbituric acid and melamine which formed highly organized molecular self-assemblies exhibiting order from the molecular scale (0.3 nm) to the macroscale (0.5 mm). This shows that macrostructures and macropatterns may be controlled by molecular functionalities.

The melamine and barbituric derivatives **1** and **2** were studied, along with **3** with a single barbituric acid for



comparison. Supramolecular assemblies were prepared by mixing **2** and **1** in a molar ratio of 1 : 2 in dried DMF ( $\sim 0.2$ – $1$  mM), followed by heating the solution to  $50$  °C for 24 h.<sup>5</sup> Samples were prepared by simply drop-casting the homogeneous solution onto various substrates such as glass, carbon, gold and germanium. These substrates were chosen to meet the requirements of various analytical techniques, for example, gold and carbon for electron microscopy and germanium for infrared spectroscopy.

The **2**·**1**<sub>2</sub> supramolecular system was linked with six complementary H-bonds ( $\sim 30$  kcal mol<sup>−1</sup>), which is the minimum number that nature requires to precisely transfer information from DNA to RNA (triplet base pairs or codons).<sup>6</sup> The formation of our supramolecular self-assemblies is driven primarily by the interplay of encoded six H-bonds, and secondarily by hydrophobic chain–chain interactions,  $\pi$ – $\pi$  interactions, and functional group–substrate interactions. The zigzag H-bond network in the **2**·**1**<sub>2</sub> system was verified with IR measurements carried out in the internal (total) reflection at the center of the flat surface of a Ge hemisphere. First, the shifts of carbonyl, amide, and amino infrared bands confirm the formation of six-fold zigzag H-bonds between **2** and **1**.<sup>7</sup>

Secondly, the carbonyl vibrations at the 2,6-position ( $1675$  cm<sup>−1</sup>) of the barbituric acid are insensitive to polarization because of their structural arrangement. However, the carbonyl vibrations at the 4-position ( $1733$ ,  $1705$  cm<sup>−1</sup>; *para* to ylidine substitution) are strong in p-polarization but weak in s-polarization. This polarization effect proves that the 4-position C=O bond is mostly perpendicular to the surface, suggesting that the extended H-bonded networks are parallel to the surface. Finally, the low CH<sub>2</sub> vibration frequencies ( $\nu = 2916$  and  $\nu_s = 2849$  cm<sup>−1</sup>) indicate that the hydrocarbon chains are highly crystalline;<sup>8</sup> this order is rather long range ( $> \mu$ m) as shown by the constant CH<sub>2</sub> vibrational frequencies when the IR beam is changed from grazing incidence ( $75^\circ$ ) to near-normal incidence ( $20^\circ$ ). While **2** is replaced with **3**, no such long-range order was observed; both CH<sub>2</sub> vibration frequencies increased by  $\sim 5$  cm<sup>−1</sup> from  $75$  to  $20^\circ$ , indicating that the alkyl chains become more disordered away from the Ge substrate.

Bright-field transmission electron microscopy (TEM) indicated that these systems consist of layered structures with very long, linear ‘ribbons’ (width =  $\sim 322$ – $644$  Å) as the secondary building blocks. High-resolution TEM and electron diffraction (Fig. 1) revealed that the layered structure had four different periodicities of  $d = 2.6$ ,  $3.7$ ,  $4.0$  and  $4.6$  Å in the plane of the substrate. Small-angle X-ray diffraction of **2**·**1**<sub>2</sub> on silicon yielded the first-order Bragg diffraction peak at  $2\theta = 1.334^\circ$ , which proved that **2**·**1**<sub>2</sub> formed multilayers with a  $d$ -spacing of  $c = 66.2$  Å along surface normal. This value agrees quite well with a  $d$ -spacing of  $c = \sim 65$  Å generated from a 3D molecular model. These results also support the IR observation that the **2**·**1**<sub>2</sub> system is a layered structure with extended H-bonded networks parallel to the substrate surface. The TEM and X-ray results are consistent with the proposed supramolecular structure illustrated in Fig. 2. Fig. 2(a) describes that the distance between barbituric acids or melamines is  $9.8$  Å<sup>9</sup> and their nearest neighbor in the next sheet is  $4.3$  Å away at an angle of  $70^\circ$ . This packing (Fig. 2) of the extended H-bond networks can explain all the observed  $d$ -spacing values;<sup>10</sup> they are (1) the periodicity along the H-bond network  $d(1,-1) = a \sin 60^\circ = 4.6$  Å, and (2) the stacking distance between H-bond networks  $d(1,1) = b \sin 32.5^\circ = 4.0$  Å and between phenyl rings in **2**

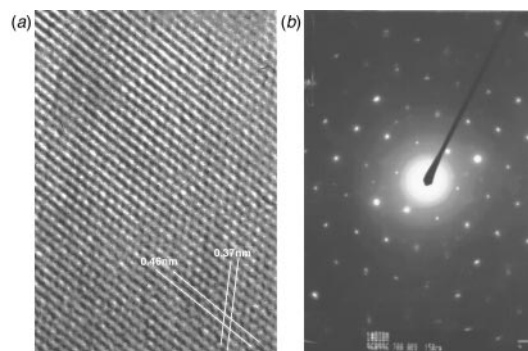


**Fig. 1** (a) A high-resolution TEM image of the **2**·**1**<sub>2</sub> multilayer supramolecular self-assembly on a carbon-coated copper grid. The four  $d = 2.6$ ,  $3.7$ ,  $4.0$  and  $4.6$  Å. (b) An electron diffraction pattern of the same **2**·**1**<sub>2</sub> system confirms the  $d$ -spacing values of  $2.6$ ,  $3.7$ ,  $4.0$  and  $4.6$  Å.

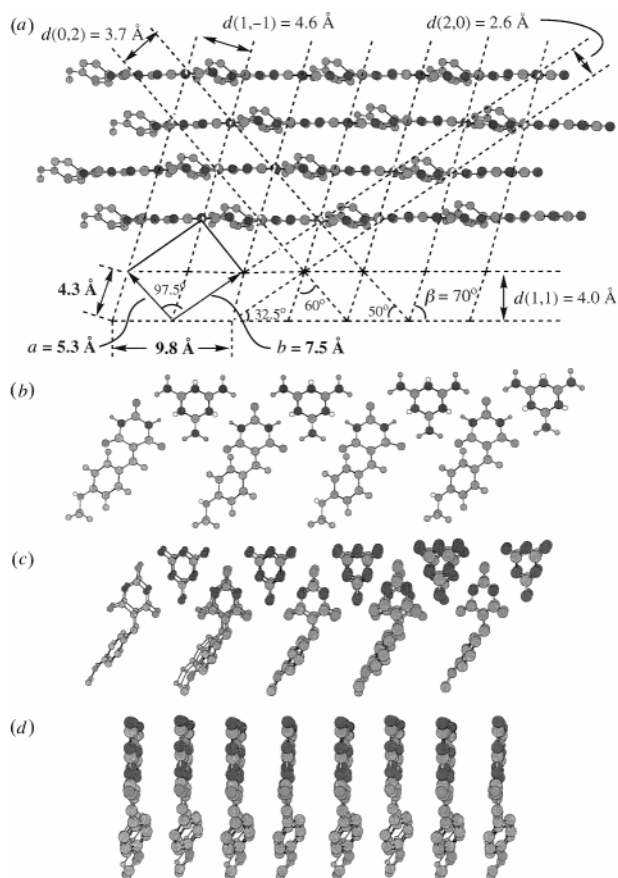


**Fig. 2** (a) Proposed  $2\cdot 1_2$  crystal lattice structure which explains the observed  $d$ -spacing values. (b) Side view of the H-bond networks,  $d(1,-1) = 4.6$  Å. (c) Stacking along the phenyl ring direction,  $d(0,2) = 3.7$  Å. (d) End view of H-bond networks, distance between H-bond sheets is  $d(1,1) = 4.0$  Å.

$d(0,2) = 3.7$  Å, and  $d(2,0) = 2.6$  Å. Molecular modeling of steric interactions between the 2,6-position oxygen atoms and the *ortho* position hydrogen atoms on the phenyl ring gives a dihedral angle between these two stacking planes of  $49^\circ$  [Fig. 2(a),(c)]. This angle corresponds to the  $50^\circ$  angle observed in high-resolution TEM between  $d(0,2) = 3.7$  Å phenyl–phenyl planes and  $d(1,1) = 4.0$  Å barbituric–melamine planes.

In Fig. 3(a), we observed that the amplified molecular information was expressed as very long straight lines with a line width between 3 and 4  $\mu\text{m}$  and a length exceeding 0.1 mm. Furthermore, the amplified molecular information stored in the chemical units also generated well-defined angular structures of  $60^\circ$  and  $70^\circ$  through intermolecular interactions. These features may result from much interplay of secondary interactions including the H-bond, ribbon packing, and the alkyl chain interaction/tilt. When we substituted **3** for **2**, no such pattern was

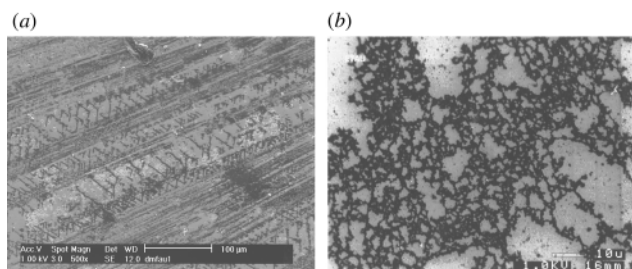


**Fig. 3** (a) SEM images of  $2\cdot 1_2$  systems on gold surfaces. The  $2\cdot 1_2$  self-assemblies are darker, and they form extremely long lines ( $>0.5$  mm) and micron-size angles. These geometric features are constructed from secondary plate-like units, which are also observed in the micrograph. (b) The SEM image of the  $3\cdot 1$  system on gold surfaces shows random network structures. Note that the  $3\cdot 1$  system has all the functionalities of the  $2\cdot 1_2$  system. The only difference is that the two barbituric acid groups are linked together in the  $2\cdot 1_2$  system.

observed [Fig. 3(b)]. This fact suggests that the template effect from the gold substrate is not a dominant factor in the formation of these specific geometric structures because **3** has all the chemical functional groups that **2** has. Furthermore, these lines are hierarchical and built from smaller dot-like units ( $0.5\text{--}2$   $\mu\text{m}$ ) which are also observed in the SEM image. The SEM micrograph clearly shows that there is a strong tendency to form such long-range ordered patterns that are governed by the information encoded in the molecular structures. These results imply that molecular building blocks can be programmed to spontaneously assemble into prescribed structures according to a molecular blueprint, a process needed in materials by design. In the  $2\cdot 1_2$  system, we have employed H-bonding interactions and hydrophobic associations to generate microscale straight lines and angles on gold surfaces. The ability to generate pattern on the microscale through tuning of the molecular functionality is important because it allows formation of unique structures without utilizing external lithographic tools.

In conclusion, we have demonstrated that molecular design can lead to order on the microscale, mesoscale, and macroscale. The results show that H-bonding effects are the major driving forces in our systems, compared to hydrophobic interactions and van der Waals forces. The perfect match of six pairs of H-bonds induces the system to spontaneously organize into highly ordered hierarchical architectures manifested as micro-wide straight lines with  $60^\circ$  and  $70^\circ$  angles.

The authors at Los Alamos National Laboratory acknowledge the support of Laboratory Directed Research and Development and Center of Materials Science. The authors at Jilin University are grateful for support from National Climbing B Project and the National Science Foundation of China.

## Notes and references

- R. P. Andres, J. D. Bielefeld, J. I. Henderson, D. B. Janes, V. R. Kolagunta and C. P. Kubiak, *Science*, 1996, **273**, 1690; D. Q. Li, M. A. Rathner, T. J. Marks, C. Zhang, J. Yang and G. K. Wong, *J. Am. Chem. Soc.*, 1990, **112**, 7389; G. E. Poirier and E. D. Pylant, *Science*, 1996, **272**, 1145; X. Yang, D. McBranch, B. I. Swanson and D. Q. Li, *Angew. Chem., Int. Ed. Engl.*, 1996, **35**, 538; R. Maoz, S. Matlis, E. Dimasi, B. M. Ocko and J. Sagiv, *Nature*, 1996, **384**, 150; V. R. Pedireddi and C. N. R. Rao, *J. Am. Chem. Soc.*, 1999, **121**, 1752.
- D. Gurrera, L. D. Taylor and J. C. Warner, *Chem. Mater.*, 1994, **6**, 1293; E. Fan, C. Vicent, S. J. Geib and A. D. Hamilton, *Chem. Mater.*, 1994, **6**, 1113.
- T. M. Bohanon, S. Denzinger, R. Fink, W. Paulus, H. Ringsdorf and M. Weck, *Angew. Chem., Int. Ed. Engl.*, 1995, **34**, 58.
- J. A. Zerkowski and G. M. Whitesides, *J. Am. Chem. Soc.*, 1994, **116**, 4298; J. M. Lehn, M. Mascal, A. Decian and J. Fischer, *J. Chem. Soc., Chem. Commun.*, 1990, 479.
- Y. W. Cao, PhD Thesis, Jilin University, Changchun, PRC, 1996.
- A. Krasnopoler, N. Kizhakevariam and E. M. Stuve, *J. Chem. Soc., Faraday Trans.*, 1996, **92**, 2445; M. W. Feyereisen, D. Feller and D. A. Dixon, *J. Phys. Chem.*, 1996, **100**, 2993.
- 2** has amide N–H vibrations at  $3217$  (vs),  $3143$  (sh) and  $3049$  (sh)  $\text{cm}^{-1}$  and carbonyl C=O absorption bands at  $1754$  (sh),  $1740$  (sh),  $1724$  (s),  $1692$  and  $1668$   $\text{cm}^{-1}$ . The stretching bands for amino groups in **1** are observed at  $3450$  (m),  $3342$  (m),  $3271$  (m) and  $3164$  (m)  $\text{cm}^{-1}$ , and the N–H deformation bands appear at  $1671$  (sh) and  $1627$  (sh)  $\text{cm}^{-1}$ . Upon self-assembly, the N–H vibrations become weak and shift to  $3329\text{--}3259$  (br) and  $3138\text{--}3126$   $\text{cm}^{-1}$ ; the carbonyl vibrations change to new positions at  $1733$  (sh),  $1705$  (s) and  $1675$  (s)  $\text{cm}^{-1}$ .
- C. W. Sheen, J.-X. Shi, J. Martensson, A. N. Parikh and D. L. Allara, *J. Am. Chem. Soc.*, 1992, **114**, 1514; D. L. Allara, S. V. Atre, C. A. Elliger and R. G. Snyder, *J. Am. Chem. Soc.*, 1991, **113**, 1852; R. G. Nuzzo, L. H. Dubois and D. L. Allara, *J. Am. Chem. Soc.*, 1990, **112**, 558.
- J. A. Zerkowski, J. C. Macdonald, C. T. Seto, D. A. Wierda and G. M. Whitesides, *J. Am. Chem. Soc.*, 1994, **116**, 2382.
- M. Mascal, P. S. Fallon, A. S. Batsanov, B. R. Heywood, S. Champ and M. Colclough, *J. Chem. Soc., Chem. Commun.*, 1995, 805; M. Mascal, N. M. Hext, R. Warmuth, M. H. Moore and J. P. Turkenburg, *Angew. Chem., Int. Ed. Engl.*, 1996, **35**, 2204.